American Journal of Information Science and Computer Engineering
Vol. 5, No. 2, 2019, pp. 47-65
http://www.aiscience.org/journal/ajisce
ISSN: 2381-7488 (Print); ISSN: 2381-7496 (Online)

An Analytical Study on Entropy Generation in the Poiseuille Flow of a Temperature Dependent Viscosity Through a Channel

Vembu Ananthaswamy[1, *], Moorthi Subha[2], Aliyar Mohamed Fathima[1]

[1]Department of Mathematics, The Madura College, Madurai, Tamil Nadu, India
[2]Department of Mathematics, MSNPM Women's College, Poovanthi, Tamil Nadu, India

Abstract

In this paper, we discuss the effects of thermal radiation on entropy generation in a temperature dependent viscosity fluid flow in a channel with a naturally permeable wall of very small permeability. A mathematical study on the isothermal and convection boundary conditions and the effects of various pertinent parameters are examined. The approximateanalytical expressions of the dimensionless velocity field, dimensionless temperature field, dimensionless entropy generation number and the dimensionless Bejan number are derived using the Homotopy analysis method. Our analytical results are compared graphically with the numerical solutions and a satisfactory agreement is noted.

Keywords

Entropy Generation, PoiseuilleFlow, Naturally Permeable, Non-linear Boundary Value Problem, Homotopy Analysis Method

Received: March 14, 2019 / Accepted: April 25, 2019 / Published online: May 13, 2019

1. Introduction

The viscous fluid flow is a subject of growing interest. Since the Pressure-driven or shear driven flows through achannels have many applications, the investigation on it is most important. It has many applications in soil mechanics, oil field operations, in transpiration cooling, lubrication of porous bearing and water purification etc. Nield and Bejan [2], have discussed such applications and many others. Instability of Poiseuille flow in a fluid overlying fluid saturated porous medium layer is investigated by Chang, Chen and Straughan [3]. Hill and Straughan [4], numerically investigates the instability of Poiseuille flow in a fluid overlying a porous medium saturated with the same fluid. Beavers and Joseph [5], examined the boundary conditions at a naturally permeable wall. The boundary condition at the surface of a porous medium is discussed by Saffman [6]. Ochoa-Tapia and Whitaker [7, 8], have investigated about Momentum transfer at the boundary between a porous medium and a homogeneous fluid.

The study of viscous fluid flow and heat transfer in channels filled or partially filled with a porous medium is important due to their recent technological improvement in engineering. David [9] have discussed in flow at the interface of a model fibrous medium. Chauhan and Shekhawat [10] examined heat transfer in couette flow of a compressible Newtonian fluid in the presence of a naturally permeable boundary. The similar geometry with partly filled by a porous medium and a transverse sinusoidal injection velocity is investigated by Chauhan and Vyas [11]. Analytical investigation was presented by Kuznetsov [12] of fluid flow in the interface region between a porous medium and a clear fluid in channels partially filled with a porous medium. Also Kuznetsov [13, 14] examined couette flow and heat transfer

* Corresponding author
E-mail address: ananthu9777@rediffmail.com (V. Ananthaswamy)

effects in a composite channel partially filled with a porous medium and partially with a clear fluid. Alkam et al. [15] investigated forced convection in channels partially filled with porous substrates.

Most of the investigations dealing with the First Law of thermodynamics. From the experimental studies it is cleared that when heat energy is transferred, only a partial energy is converted to work. Bejan [17] studied entropy generation in thermal systems and investigated the importance of entropy minimization in improving their performance. Chen et al. [18], discussed effects of thermal radiation on entropy generation due to flow along wavy or flat plate.

The aim of this paper is to analyse the mathematical expressions of the entropy generation in Poiseuille flow of a fluid overlying a porous medium under thermal radiation. The approximateanalytical expressions of the dimensionless velocity profiles, dimensionless temperature profiles, dimensionless entropy generation number and the dimensionless Bejan number are derived using the Homotopy analysis method and discussed by graphically.

2. Mathematical Formulation of the Problem

We consider the flow of fluid with temperature dependent viscosity through a horizontal parallel channel of width *'d'*. The upper wall of the channel is impermeable, while the lower wall is a naturally permeable medium of very small permeability and saturated with fluid at constant temperature$'T_0'$.

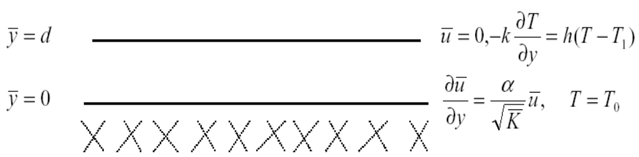

Figure 1. Schematic diagram for fluid flow.

The flow in the bounding porous medium wall is modelled by the Darcy's equation therefore in the absence of any external pressure gradient, the filter velocity in the porous matrix of very small permeability is assumed to be zero. The effect of the porous matrix is, thus to introduce a velocity slip at the lower bounding wall of the channel and its permeability affects flow in the channel through Saffman slip boundary condition [6]. The flow in the parallel wall channel is driven by a constant pressure gradient applied at the mouth of the channel. The upper impermeable channel wall is assumed to have a negligible thickness and its upper face is in contact with another fluid at temperature$'T_1'$. The upper wall is thus heated by convection from external hot fluid which provides a convection heat transfer coefficient *'h'*.

Further it is assumed that property variations of the viscous fluid in the channel because of temperature are limited to only, which is assumed to vary as an inverse linear function of temperature, following Lai and Kulacki [31], as follows viscosity:

$$\mu(T) = \frac{\mu_0}{1+\lambda(T-T_0)} \tag{1}$$

where μ_0, is the viscosity of the fluid at the temperature T_0, and λ is the viscosity variation parameter. The governing equations for the present problem are given by

$$\frac{\partial \bar{u}}{\partial \bar{x}} = 0 \tag{2}$$

$$\frac{\partial}{\partial \bar{y}}\left(\mu(T)\frac{\partial \bar{u}}{\partial \bar{y}}\right) - \frac{\partial \bar{p}}{\partial \bar{x}} = 0 \tag{3}$$

$$\frac{k}{\rho C_P}\left(\frac{\partial^2 T}{\partial \bar{y}^2}\right) + \frac{\mu(T)}{\rho C_P}\left(\frac{\partial \bar{u}}{\partial \bar{y}}\right)^2 - \frac{1}{\rho C_P}\frac{\partial q_r}{\partial \bar{y}} = 0 \tag{4}$$

The corresponding boundary conditions are given by

$$\frac{\partial \bar{u}}{\partial \bar{y}} = \frac{\alpha}{\sqrt{K}}\bar{u}, \quad T = T_0 \quad when \ \bar{y} = 0 \tag{5}$$

$$\bar{u} = 0, \ -k\frac{\partial T}{\partial \bar{y}} = h(T - T_1) \quad when \ \bar{y} = d \tag{6}$$

where, $\bar{u}$ is the velocity in the x-direction; T is the temperature; ρ, the density; C_P, the specific heat at the constant pressure; k, the thermal conductivity;

$-\frac{\partial \bar{p}}{\partial \bar{x}}$, the pressure gradient; and $\mu(T)$, the temperature dependent viscosity of the fluid; $\overline{K}$, the permeability of the porous medium; and α, the dimensionless constant depending on the local geometry of interstices of the porous matrix.

In this study, the Rosseland diffusion flux model is taken to simulate radiative heat transfer which is suitable for an optical thick fluid and gray, absorbing-emitting, but not scattering medium. Following Siegel and Howell [32], it takes the form

$$q_r = -\frac{4\sigma}{3k_1}\frac{\partial T^4}{\partial \bar{y}} \tag{7}$$

where σ, the Stefan-Boltzmann constant; and k_1, the mean absorption coefficient. The term T^4 can be expanded for small temperature differences in a Taylor series about T_0 as follows $T^4 = T_0^4 + (T - T_0)4T_0^3 = 4T_0^3 T - 3T_0^4$, and neglecting higher terms:

Thus, we have

$$q_r = -\frac{16\sigma T_0^3}{3k_1}\frac{\partial T}{\partial \bar{y}} \tag{8}$$

Let us introduce the dimensionless quantities are as follows:

$$u = \frac{\bar{u}}{U},\ x = \frac{\bar{x}}{d},\ y = \frac{\bar{y}}{d},\ \theta = \frac{T - T_0}{T_1 - T_0},\ P = \frac{d^2}{\mu_0 U}\left(-\frac{\partial \bar{P}}{\partial \bar{x}}\right),\ K = \frac{\bar{K}}{d^2},\ a = \lambda(T - T_0) \tag{9}$$

Substituting the eqns. (1), (7) and (8) intothe eqns. (2)-(5), we obtain the governing eqns. in dimensionless form are as follows:

$$\frac{du}{dx} = 0 \tag{10}$$

$$\frac{d}{dy}\left(\frac{1}{(1+a\theta)}\frac{du}{dy}\right) = -P \tag{11}$$

$$\frac{d^2\theta}{dy^2} + \left(\frac{3N_R}{4+3N_R}\right)\frac{Br}{(1+a\theta)}\left(\frac{du}{dy}\right)^2 = 0 \tag{12}$$

The corresponding boundary conditions are given by

$$\frac{du}{dy} = \frac{\alpha}{\sqrt{K}}u,\quad \theta = 0 \text{ when } y = 0 \tag{13}$$

$$u = 0,\quad \frac{d\theta}{dy} = -Bi(\theta - 1) \text{ when } y = 1 \tag{14}$$

where, P is the dimensionless axial pressure gradient; U, the flow characteristic velocity;a nd a, the variable viscosity parameter. For constant viscosity case we have $a = 0$; and for $a > 0$, the viscosity ofthe fluid decreases with rise in temperature.

Here N_R, represents the Stark number; Br, isthe Brinkman number; Bi, is the Biot number, K, is the Permeability parameter.

The dimensionless entropy number [1] can be defined as follows:

$$NS = \left(\frac{4+3N_R}{3N_R}\right)\left(\frac{d\theta}{dy}\right)^2 + \frac{B_r}{\Omega(1+a\theta)}\left(\frac{du}{dy}\right)^2 \tag{15}$$

$$NS = NS_1 + NS_2 \tag{16}$$

where $\Omega = \frac{\Delta T}{T'}$, the dimensionless temperature difference; NS_1 is the dimensionless entropy generation due to heat transfer in the presence of radiation; and NS_2, the dimensionless entropy generation due to fluid friction.

The dimensionless Bejan number *(Be)*[1] can be defined by

$$Be = \frac{NS_1}{NS} = \frac{Entropy\ generation\ due\ to\ heat\ transfer}{Total\ Entropy\ generation} \tag{17}$$

3. Solution of the Problem using the Homotopy Analysis Method

This section deals with a basic strong analytic tool for non-linear problems, namely the Homotopy analysis method (HAM) which was generated by Liao [19], is employed to solve the nonlinear differential eqns. (10) – (12). The Homotopy analysis method is based on a basic concept in topology. Unlikeperturbation techniques like [20], the Homotopy analysis method is independent of the small/large parameters. Unlike all other reported perturbation and non-perturbation techniques such as the artificial small parameter method [21], the δ-expansion method [22] and Adomian's decomposition method [23], the Homotopy analysis method provides us a simple way to adjust and control the convergence region and rate of approximation series. The Homotopy analysis method has been successfully applied to many nonlinear problems such as heat transfer [24], viscous flows [25], nonlinear oscillations [26], Thomas-Fermi's atom model [27], nonlinear water waves [28], etc. Such varied successful applications of the Homotopy analysis method confirm its validity for nonlinear problems in science and engineering. The Homotopy analysis method is a good technique when compared to other perturbation methods. The existence of the auxiliary parameter h in the Homotopy analysis method provides us with a simple way to adjust and control the convergence region of the solution series.

3.1. Basic Concepts of the Homotopy Analysis Method

Consider the following differential equation:

$$N\left[u(t)\right] = 0 \tag{18}$$

where N is a nonlinear operator, t denotes an independent variable, $u(t)$ is an unknown function. Forsimplicity, weignore all boundary or initial conditions, which can be treated in the similar way. By means of generalizing the conventional Homotopy method, Liao constructed the so-called zero-order deformation equation as:

$$(1-p)L\left[\phi(t;p)-u_0(t)\right]=p\,h\,H(t)N\left[\phi(t;p)\right] \quad (19)$$

where $p\in[0,1]$ is the embedding parameter, $h\neq 0$ is a nonzero auxiliary parameter, $H(t)\neq 0$ is an auxiliary function, L an auxiliary linear operator, $u_0(t)$ is an initial guess of $u(t),\phi(t;p)$ is an unknown function. It is important to note that one has great freedom to choose auxiliary unknowns in HAM. Obviously, when p = 0 and p =1, it holds:

$$\phi(t;0)=u_0(t) \text{ and } \phi(t;1)=u(t) \quad (20)$$

respectively. Thus, as p increases from 0 to 1, the solution $\phi(t;p)$ varies from the initial guess $u_0(t)$ to the solution $u(t)$.

Expanding $\phi(t;p)$ in Taylor series with respect to p, we have:

$$\phi(t;p)=u_0(t)+\sum_{m=1}^{+\infty}u_m(t)p^m \quad (21)$$

$$u_m(t)=\frac{1}{m!}\frac{\partial^m\phi(t;p)}{\partial p^m} \quad (22)$$

If the auxiliary linear operator, the initial guess, the auxiliary parameter h, and the auxiliary function are so properly chosen, the series eqn. (19) converges at $p=1$ then we have:

$$u(t)=u_0(t)+\sum_{m=1}^{+\infty}u_m(t) \quad (23)$$

Differentiating the eqn. (17) for m times with respect to the embedding parameter p, and then setting $p=0$ and finallydividing them by m!, we will have so-called $m\,th$ order deformation equation as:

$$L\left[u_m-\chi_m u_{m-1}\right]=h\,H(t)\Re_m\left(\vec{u}_{m-1}\right) \quad (24)$$

where

$$\Re_m\left(\vec{u}_{m-1}\right)=\frac{1}{(m-1)!}\frac{\partial^{m-1}N\left[\phi(t:p)\right]}{\partial p^{m-1}} \quad (25)$$

And

$$\chi_m=\begin{cases}0, & m\le 1,\\ 1, & m>1.\end{cases} \quad (26)$$

Applying L^{-1} on both side of eqn. (22), we get

$$u_m(t)=\chi_m u_{m-1}(t)+hL^{-1}\left[H(t)\Re_m\left(\vec{u}_{m-1}\right)\right] \quad (27)$$

In this way, it is easily to obtain u_m for $m\ge 1$, at M^{th} order, we have

$$u(t)=\sum_{m=0}^{M}u_m(t) \quad (28)$$

when $M\to+\infty$, we get an accurate approximation of the original eqn. (16). For the convergence of the above method we refer the reader to Liao [19]. If the eqn. (16) admits unique solution, then this method will produce the unique solution.

3.2. Approximate Analytical Expressions of the Non-linear Differential Eqns. (10) and (11) using Homotopy Analysis Method

$$\frac{d}{dy}\left(\frac{1}{(1+a\theta)}\frac{du}{dy}\right)=-P \quad (29)$$

$$\frac{d^2\theta}{dy^2}+\left(\frac{3N_R}{4+3N_R}\right)\frac{Br}{(1+a\theta)}\left(\frac{du}{dy}\right)^2=0 \quad (30)$$

We construct Homotopy for the eqns. (27) and (28) are as follows:

$$(1-p)\left(\frac{d^2u}{dy^2}+P\right)-hw\left[\frac{d^2u}{dy^2}(1+a\theta)+\frac{du}{dy}(-a)\frac{d\theta}{dy}+P\right]=0 \quad (31)$$

$$(1-p)\left(\frac{d^2\theta}{dy^2}\right)-hp\left[\frac{d^2\theta}{dy^2}(1+a\theta)+\left(\frac{3N_R}{4+3N_R}\right)Br\left(\frac{du}{dy}\right)^2\right]=0 \quad (32)$$

The approximate solution of the eqns. (29) and (30) are as follows:

$$u = u_0 + pu_1 + p^2 u_2 + p^3 u_3 + ... \tag{33}$$

$$\theta = \theta_0 + p\theta_1 + p^2\theta_2 + p^3\theta_3 + ... \tag{34}$$

The initial approximations areas follows:

$$\frac{du_0(0)}{dy} = \frac{\alpha}{\sqrt{K}} u_0(0), \quad \theta_0(0) = 0 \tag{35}$$

$$\frac{du_i(0)}{dy} = \frac{\alpha}{\sqrt{K}} u_i(0), \quad \theta_i(0) = 0, \; i = 1,2,3..... \tag{36}$$

$$u_0(1) = 0, \quad \frac{d\theta_0(1)}{dy} = -Bi\left(\theta_0(1) - 1\right) \tag{37}$$

$$u_i(1) = 0, \quad \frac{d\theta_i(1)}{dy} = -Bi\,\left(\theta_i(1)\right), \; i = 1,2,3,....... \tag{38}$$

Substituting the eqns. (33) and (34) into the eqns. (31) and (32) we get,

$$(1-p)\left(\frac{d^2}{dy^2}(u_0 + pu_1 + ...) + P\right) - hp\begin{bmatrix} \frac{d^2}{dy^2}(u_0 + pu_1 + ...)(1 + a\theta) \\ + \frac{d}{dy}(u_0 + pu_1 + ...)(-a)\frac{d\theta}{dy} + P \end{bmatrix} = 0 \tag{39}$$

$$(1-p)\left(\frac{d^2}{dy^2}(\theta_0 + p\theta_1 + ...)\right) - hp\begin{bmatrix} \frac{d^2}{dy^2}(\theta_0 + p\theta_1 + ...)\left(1 + a\left(\theta_0 + p\theta_1 + ...\right)\right) \\ + \left(\frac{3N_R}{4 + 3N_R}\right) Br \left(\frac{du}{dy}\right)^2 \end{bmatrix} = 0 \tag{40}$$

Comparing the coefficients of p^0, p^1 in the eqns. (39) and (40) we get the following eqns.

$$p^0 : \frac{d^2 u_0}{dy^2} + P = 0 \tag{41}$$

$$p^0 : \frac{d^2\theta_0}{dy^2} = 0 \tag{42}$$

$$p^1 : \frac{d^2 u_1}{dy^2} - \frac{d^2 u_0}{dy^2} - P - h\left[\frac{d^2 u_0}{dy^2} + \frac{d^2 u_0}{dy^2} a\theta_0 - \frac{du_0}{dy} a + \frac{d\theta_0}{dy} + P\right] = 0 \tag{43}$$

$$p^1 : -\frac{d^2\theta_0}{dy^2} - h\left[\frac{d^2\theta_0}{dy^2} + a\theta_0 \frac{d^2\theta_0}{dy^2} + \left(\frac{3N_R}{4 + 3N_R}\right) Br \left(\frac{du_0}{dy}\right)^2\right] = 0 \tag{44}$$

Solving the eqns. (41) – (44) with the help of the eqns. (35)-(38), we get the following results:

$$u_0 = -\frac{py^2}{2} + \frac{\alpha P y}{2\sqrt{K}\left(1 + \frac{\alpha}{\sqrt{K}}\right)} + \frac{P}{2\left(1 + \frac{\alpha}{\sqrt{K}}\right)} \tag{45}$$

$$u_1 = -h\left[\begin{array}{l} \dfrac{1}{4}\dfrac{\alpha P a y^2}{\sqrt{K}\left(1+\dfrac{\alpha}{\sqrt{K}}\right)}\dfrac{Bi}{(1+Bi)} - \dfrac{aPy^3}{3}\dfrac{Bi}{(1+Bi)} - \dfrac{pa^2y^4}{12}\dfrac{Bi^2}{(1+Bi)^2} \\ + \dfrac{\left(-\dfrac{1}{4}\dfrac{\alpha P a}{\sqrt{K}\left(1+\dfrac{\alpha}{\sqrt{K}}\right)}\dfrac{Bi}{(1+Bi)} + \dfrac{aP}{3}\dfrac{Bi}{(1+Bi)} + \dfrac{pa^2}{12}\dfrac{Bi^2}{(1+Bi)^2}\right)}{\left(1+\dfrac{\alpha}{\sqrt{K}}\right)} \\ + \dfrac{\alpha y\left(-\dfrac{1}{4}\dfrac{\alpha P a}{\sqrt{K}\left(1+\dfrac{\alpha}{\sqrt{K}}\right)}\dfrac{Bi}{(1+Bi)} + \dfrac{aP}{3}\dfrac{Bi}{(1+Bi)} + \dfrac{pa^2}{12}\dfrac{Bi^2}{(1+Bi)^2}\right)}{\sqrt{K}\left(1+\dfrac{\alpha}{\sqrt{K}}\right)} \end{array}\right] \tag{46}$$

$$\theta_0 = \frac{Bi}{(1+Bi)}y \tag{47}$$

$$\theta_1 = -h\left[\begin{array}{l} \dfrac{-1}{4}\dfrac{N_R B_r}{(4+3N_R)}\dfrac{\left(-Py+\dfrac{\alpha P}{2\sqrt{K}\left(1+\dfrac{\alpha}{\sqrt{K}}\right)}\right)^4}{P^2} \\ +\dfrac{1}{4}\dfrac{Bi}{(1+Bi)}\dfrac{N_R B_r}{(4+3N_R)}\dfrac{\left(-P+\dfrac{\alpha P}{2\sqrt{K}\left(1+\dfrac{\alpha}{\sqrt{K}}\right)}\right)^4 y}{P^2} \\ -\dfrac{1}{64}\dfrac{Bi}{(1+Bi)}\dfrac{N_R B_r}{(4+3N_R)}\dfrac{yP^2\alpha^4}{K^2\left(1+\dfrac{\alpha}{\sqrt{K}}\right)^4} \\ -\dfrac{Bi}{(1+Bi)}\dfrac{N_R B_r}{(4+3N_R)}\dfrac{\left(-P+\dfrac{\alpha P}{2\sqrt{K}\left(1+\dfrac{\alpha}{\sqrt{K}}\right)}\right)^3 y}{P} \\ +\dfrac{1}{64}\dfrac{N_R B_r}{(4+3N_R)}\dfrac{P^2\alpha^4}{K^2\left(1+\dfrac{\alpha}{\sqrt{K}}\right)^4} \end{array}\right] \tag{48}$$

According to the HAM, we can conclude that

$$u = \lim_{p\to 1} u(y) = u_0 + u_1 \tag{49}$$

$$\theta = \lim_{p\to 1} \theta(y) = \theta_0 + \theta_1 \tag{50}$$

Using the eqns. (45) and (46) into an eqn. (49) and using the eqns. (47) and (48) into an eqn. (50) we get the following:

$$u(y)=-\frac{py^2}{2}+\frac{\alpha Py}{2\sqrt{K}\left(1+\frac{\alpha}{\sqrt{K}}\right)}+\frac{P}{2\left(1+\frac{\alpha}{\sqrt{K}}\right)}-h\left[\begin{array}{l}\frac{1}{4}\frac{\alpha Pay^2}{\sqrt{K}\left(1+\frac{\alpha}{\sqrt{K}}\right)}\frac{Bi}{(1+Bi)}-\frac{aPy^3}{3}\frac{Bi}{(1+Bi)}-\frac{pa^2y^4}{12}\frac{Bi^2}{(1+Bi)^2}\\ +\frac{\left(-\frac{1}{4}\frac{\alpha Pa}{\sqrt{K}\left(1+\frac{\alpha}{\sqrt{K}}\right)}\frac{Bi}{(1+Bi)}+\frac{aP}{3}\frac{Bi}{(1+Bi)}+\frac{pa^2}{12}\frac{Bi^2}{(1+Bi)^2}\right)}{\left(1+\frac{\alpha}{\sqrt{K}}\right)}\\ +\frac{\alpha y\left(-\frac{1}{4}\frac{\alpha Pa}{\sqrt{K}\left(1+\frac{\alpha}{\sqrt{K}}\right)}\frac{Bi}{(1+Bi)}+\frac{aP}{3}\frac{Bi}{(1+Bi)}+\frac{pa^2}{12}\frac{Bi^2}{(1+Bi)^2}\right)}{\sqrt{K}\left(1+\frac{\alpha}{\sqrt{K}}\right)}\end{array}\right] \quad (51)$$

$$\theta(y)=\frac{Bi}{(1+Bi)}y-h\left[\begin{array}{l}\frac{-1}{4}\frac{N_RB_r}{(4+3N_R)}\frac{\left(-Py+\frac{\alpha P}{2\sqrt{K}\left(1+\frac{\alpha}{\sqrt{K}}\right)}\right)^4}{P^2}\\ +\frac{1}{4}\frac{Bi}{(1+Bi)}\frac{N_RB_r}{(4+3N_R)}\frac{\left(-P+\frac{\alpha P}{2\sqrt{K}\left(1+\frac{\alpha}{\sqrt{K}}\right)}\right)^4y}{P^2}\\ -\frac{1}{64}\frac{Bi}{(1+Bi)}\frac{N_RB_r}{(4+3N_R)}\frac{yP^2\alpha^4}{K^2\left(1+\frac{\alpha}{\sqrt{K}}\right)^4}\\ -\frac{Bi}{(1+Bi)}\frac{N_RB_r}{(4+3N_R)}\frac{\left(-P+\frac{\alpha P}{2\sqrt{K}\left(1+\frac{\alpha}{\sqrt{K}}\right)}\right)^3y}{P}\\ +\frac{1}{64}\frac{N_RB_r}{(4+3N_R)}\frac{P^2\alpha^4}{K^2\left(1+\frac{\alpha}{\sqrt{K}}\right)^4}\end{array}\right] \quad (52)$$

$$\frac{d\theta}{dy}=\frac{Bi}{(1+Bi)}-h\left[\begin{array}{l}\dfrac{N_RB_r}{(4+3N_R)}\dfrac{\left(-Py+\dfrac{\alpha P}{2\sqrt{K}\left(1+\dfrac{\alpha}{\sqrt{K}}\right)}\right)^3}{P^2}\\ +\dfrac{1}{4}\dfrac{Bi}{(1+Bi)}\dfrac{N_RB_r}{(4+3N_R)}\dfrac{\left(-P+\dfrac{\alpha P}{2\sqrt{K}\left(1+\dfrac{\alpha}{\sqrt{K}}\right)}\right)^4}{P^2}\\ -\dfrac{1}{64}\dfrac{Bi}{(1+Bi)}\dfrac{N_RB_r}{(4+3N_R)}\dfrac{P^2\alpha^4}{K^2\left(1+\dfrac{\alpha}{\sqrt{K}}\right)^4}\\ -\dfrac{Bi}{(1+Bi)}\dfrac{N_RB_r}{(4+3N_R)}\dfrac{\left(-P+\dfrac{\alpha P}{2\sqrt{K}\left(1+\dfrac{\alpha}{\sqrt{K}}\right)}\right)^3}{P}\end{array}\right] \tag{53}$$

$$\frac{du}{dy}=-py+\frac{\alpha P}{2\sqrt{K}\left(1+\dfrac{\alpha}{\sqrt{K}}\right)}-h\left[\begin{array}{l}\dfrac{1}{2}\dfrac{\alpha Pay}{\sqrt{K}\left(1+\dfrac{\alpha}{\sqrt{K}}\right)}\dfrac{Bi}{(1+Bi)}-\dfrac{3aPy^2}{3}\dfrac{Bi}{(1+Bi)}-\dfrac{pa^2y^3}{3}\dfrac{Bi^2}{(1+Bi)^2}\\ +\dfrac{\alpha\left(-\dfrac{1}{4}\dfrac{\alpha Pa}{\sqrt{K}\left(1+\dfrac{\alpha}{\sqrt{K}}\right)}\dfrac{Bi}{(1+Bi)}+\dfrac{aP}{3}\dfrac{Bi}{(1+Bi)}+\dfrac{pa^2}{12}\dfrac{Bi^2}{(1+Bi)^2}\right)}{\sqrt{K}\left(1+\dfrac{\alpha}{\sqrt{K}}\right)}\end{array}\right] \tag{54}$$

Substituting the eqns. (53) and (54) into the eqn. (15), we get the analytical expression of entropy generation number NS.

$$NS_1=\left(\frac{4+3N_R}{3N_R}\right)\left(\frac{Bi}{(1+Bi)}-h\left[\begin{array}{l}\dfrac{N_RB_r}{(4+3N_R)}\dfrac{\left(-Py+\dfrac{\alpha P}{2\sqrt{K}\left(1+\dfrac{\alpha}{\sqrt{K}}\right)}\right)^3}{P^2}\\ +\dfrac{1}{4}\dfrac{Bi}{(1+Bi)}\dfrac{N_RB_r}{(4+3N_R)}\dfrac{\left(-P+\dfrac{\alpha P}{2\sqrt{K}\left(1+\dfrac{\alpha}{\sqrt{K}}\right)}\right)^4}{P^2}\\ -\dfrac{1}{64}\dfrac{Bi}{(1+Bi)}\dfrac{N_RB_r}{(4+3N_R)}\dfrac{P^2\alpha^4}{K^2\left(1+\dfrac{\alpha}{\sqrt{K}}\right)^4}\\ -\dfrac{Bi}{(1+Bi)}\dfrac{N_RB_r}{(4+3N_R)}\dfrac{\left(-P+\dfrac{\alpha P}{2\sqrt{K}\left(1+\dfrac{\alpha}{\sqrt{K}}\right)}\right)^3}{P}\end{array}\right]\right)^2 \tag{55}$$

$$NS_2 = \frac{B_r}{\Omega(1+a\theta)}\left(py + \frac{\alpha P}{2\sqrt{K}\left(1+\frac{\alpha}{\sqrt{K}}\right)} - h\left[\frac{1}{2}\frac{\alpha Pay}{\sqrt{K}\left(1+\frac{\alpha}{\sqrt{K}}\right)}\frac{Bi}{(1+Bi)} - \frac{3aPy^2}{3}\frac{Bi}{(1+Bi)} - \frac{pa^2y^3}{3}\frac{Bi^2}{(1+Bi)^2} + \frac{\alpha\left(-\frac{1}{4}\frac{\alpha Pa}{\sqrt{K}\left(1+\frac{\alpha}{\sqrt{K}}\right)}\frac{Bi}{(1+Bi)} + \frac{aP}{3}\frac{Bi}{(1+Bi)} + \frac{pa^2}{12}\frac{Bi^2}{(1+Bi)^2}\right)}{\sqrt{K}\left(1+\frac{\alpha}{\sqrt{K}}\right)} \right] \right)^2 \quad (56)$$

Substituting the eqns. (55) and (56) into the eqns. (16) we get the analytical expression of entropy generation number NS. And substituting the eqn. (55) and the entropy generation number NS into the eqn. (17) we get the analytical expression of the Bejan number Be.

4. Results and Discussion

Figure 1 shows geometry of the problem. Figures 2-4 represents dimensionless velocity *u(y)* versus dimensionless distance y. From Figure 2, it is noted thatthe velocity increases when the Permeability parameter K increases, and in some fixed values of the other dimensionless parameters. From Figure 3, it is inferred that when the variable viscosity parameter a increases the corresponding velocity also increases in some fixed values of the other parameters. From Figure 4, it is depict that when the Biot number Bi *i*ncreases the corresponding velocity also increases, in some fixed values of the other dimensionless parameters.

Figures 5-9 represents the dimensionless temperature $\theta(y)$ versus the dimensionless distance y. From Figure 5, it is noted that the temperature increases when the Permeability parameter K increases, and in some fixed values of the other dimensionless parameters. From Figure 6, it is inferred that when the variable viscosity parameter a increases, the corresponding temperature also increases in some fixed values of the other dimensionless parameters. From Figure 7, it is depicting that when the Brinkman number $B_r$increases. thecorresponding temperature also increases, in some fixed values of the other dimensionless parameters. From Figure 8, it is noted that the temperature increases when the Stark number N_R increases, and in some fixed values of the other dimensionless parameters. From Figure 9, it is inferred that when the Biot number B_i increases, the corresponding temperature also increases in some fixed values of the other dimensionless parameters.

Figures 10-13 represents dimensionless entropy generation NS versus dimensionless distance y. From Figure 10, it is noted that the entropy generation increases, the permeability parameter K increases, and in some fixed values of the other dimensionless parameters. From Figure 11, it is inferred that when the Biot number B_i increases, the corresponding entropy generation also increases in some fixed values of the other dimensionless parameters. From Figure 12, it is inferred that when the temperature difference Ωincreases the corresponding entropy generation decreases in some fixed values of the other dimensionless parameters. From Figure 13, it is depict that when the axial pressure gradient Pincreases, the corresponding entropy generation also increases in some fixed values of the other dimensionless parameters.

Figures 14-18 represents Bejan number *(Be)* versus dimensionless distance y. From Figure 14, it is noted that the when the Bejan number Be increases, the Permeability parameter K increases, and in some fixed values of the other dimensionless parameters. From Figure 15, it is inferred that when the Brinkman number B_r increases, the corresponding Bejan number decreases in some fixed values of the other dimensionless parameters. From Figure 16, it depicts that when the Biot number B_i increases, the corresponding Bejan number also increases in some fixed values of the other parameters. From Figure 17, it is inferred that when the temperature difference Ω increases, the corresponding Bejan number also increases in some fixed values of the other dimensionless parameters. From Figure 18, it is depict that when the axial pressure gradient P increases, the corresponding Bejan number decreases in some fixed values of the other dimensionless parameters.

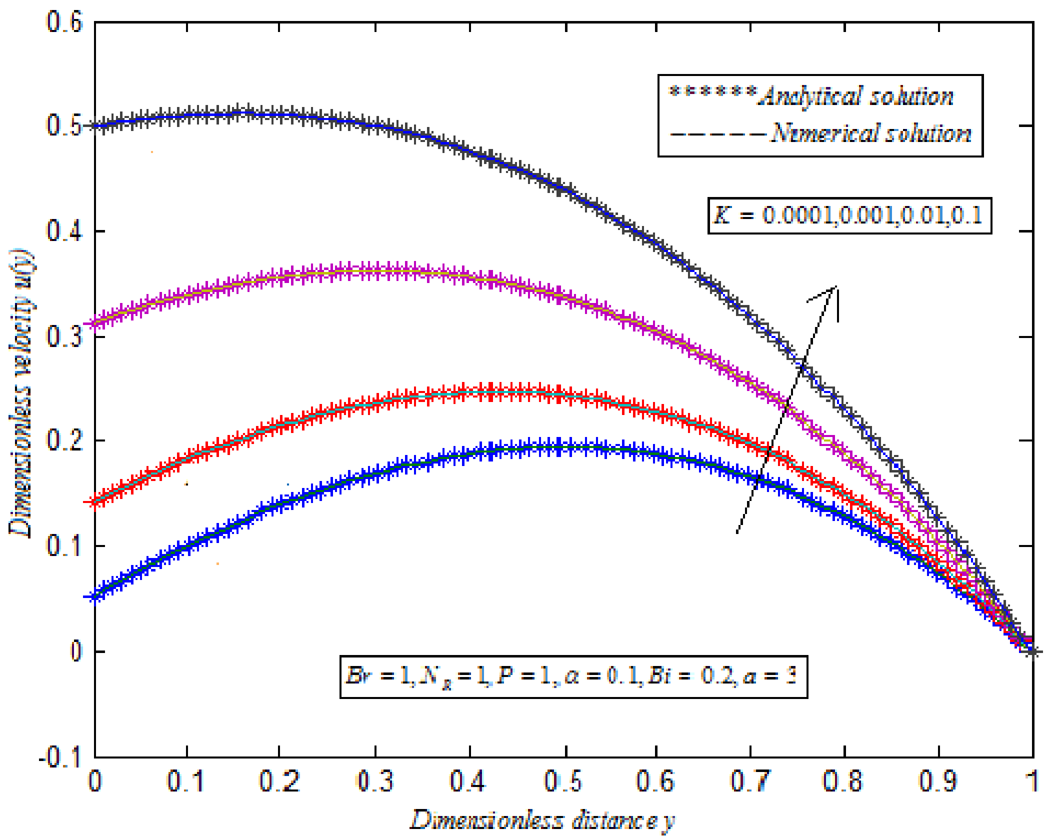

Figure 2. Dimensionless velocity *u(y)* versus the dimensionless distance *y*. The curves are plotted using the eqn. (51) for various values of the Permeability parameter *K*, and in some fixed values of the other dimensionless parameters $B_r, N_R, P, \alpha, Bi, a$.

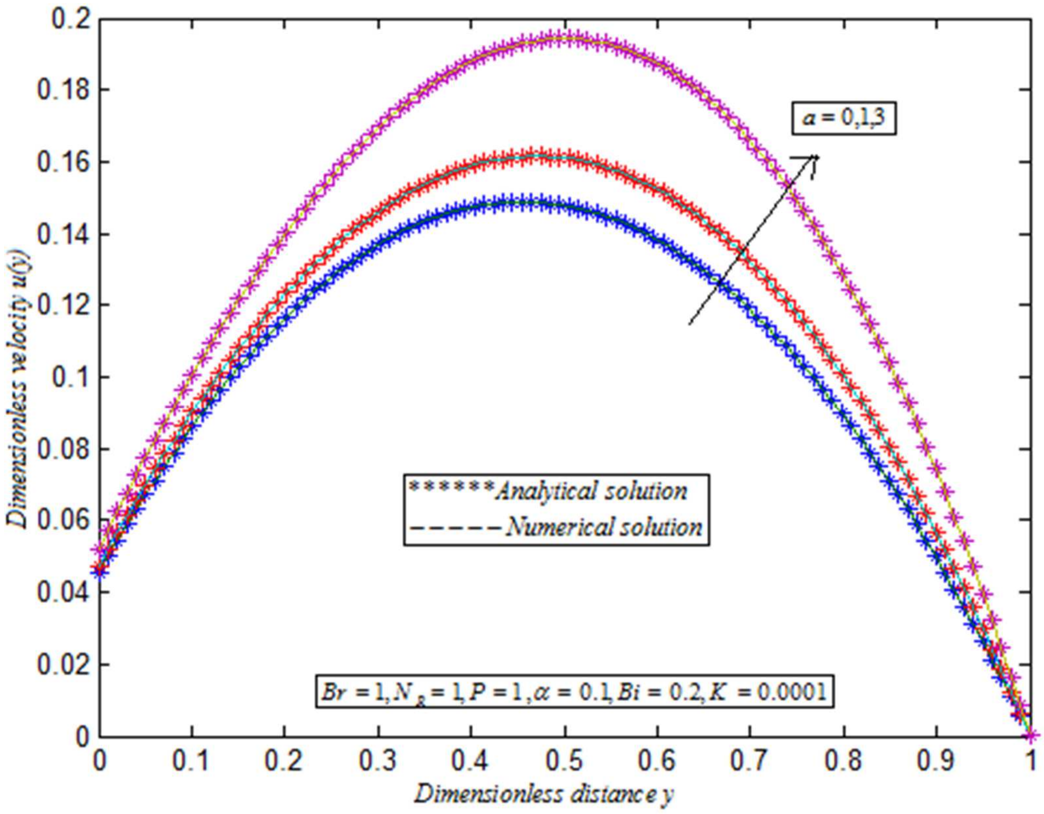

Figure 3. Dimensionless velocity *u(y)* versusdimensionless distance *y*. The curves are plotted using the eqn. (51) for various values of the variable viscosity parameter a , and in some fixed values of the other dimensionless parameters $B_r, N_R, P, \alpha, Bi, K$.

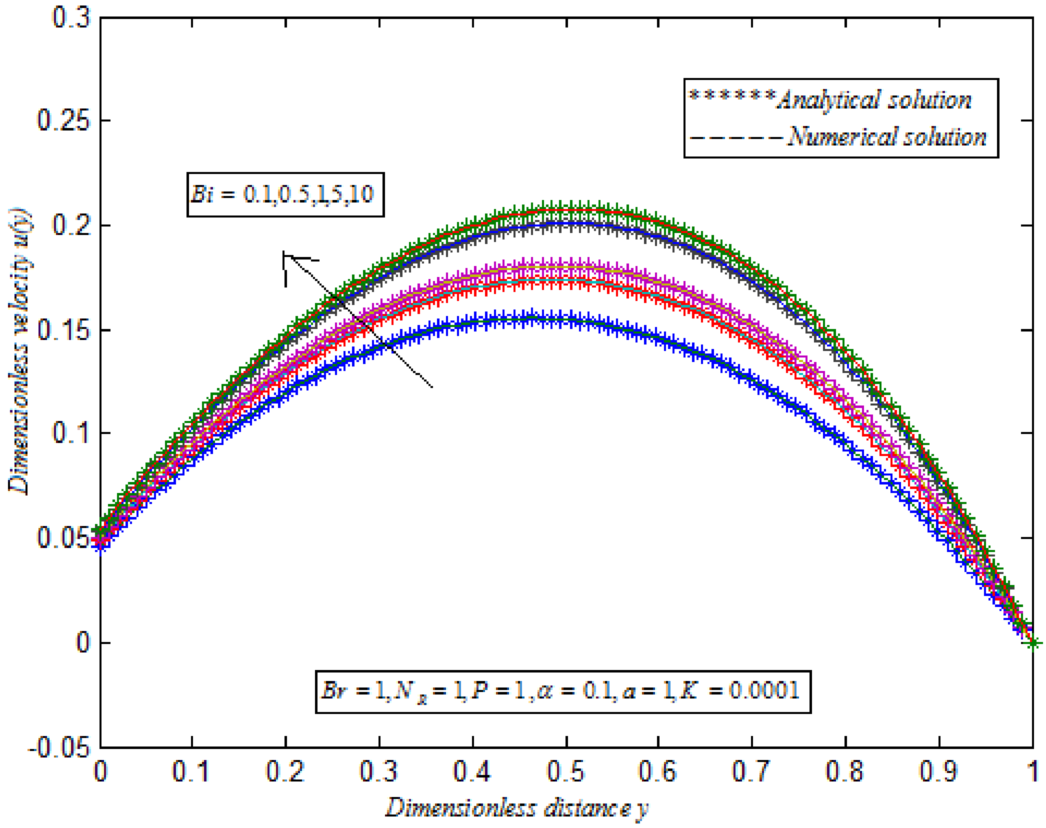

Figure 4. Dimensionless velocity *u(y)* versus dimensionless distance *y*. The curves are plotted using the eqn. (51) for various values of the Biot number *Bi*, and in some fixed values of the other dimensionless parameters $B_r, N_R, P, a, \alpha, K$.

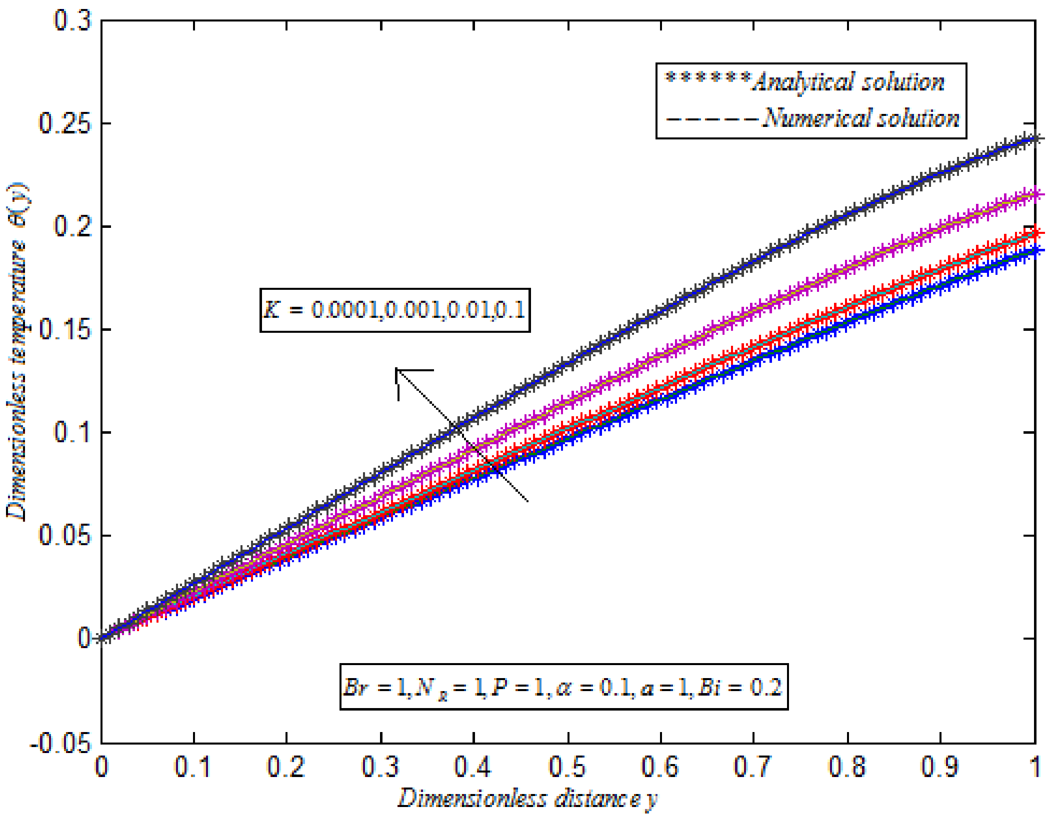

Figure 5. Dimensionless temperature $\theta(y)$ versus dimensionless distance *y*. The curves are plotted using the eqn. (52) for various values of the permeability parameter *K*, and in some fixed values of the other dimensionless parameters $P, N_R, Br, \alpha, Bi, a$.

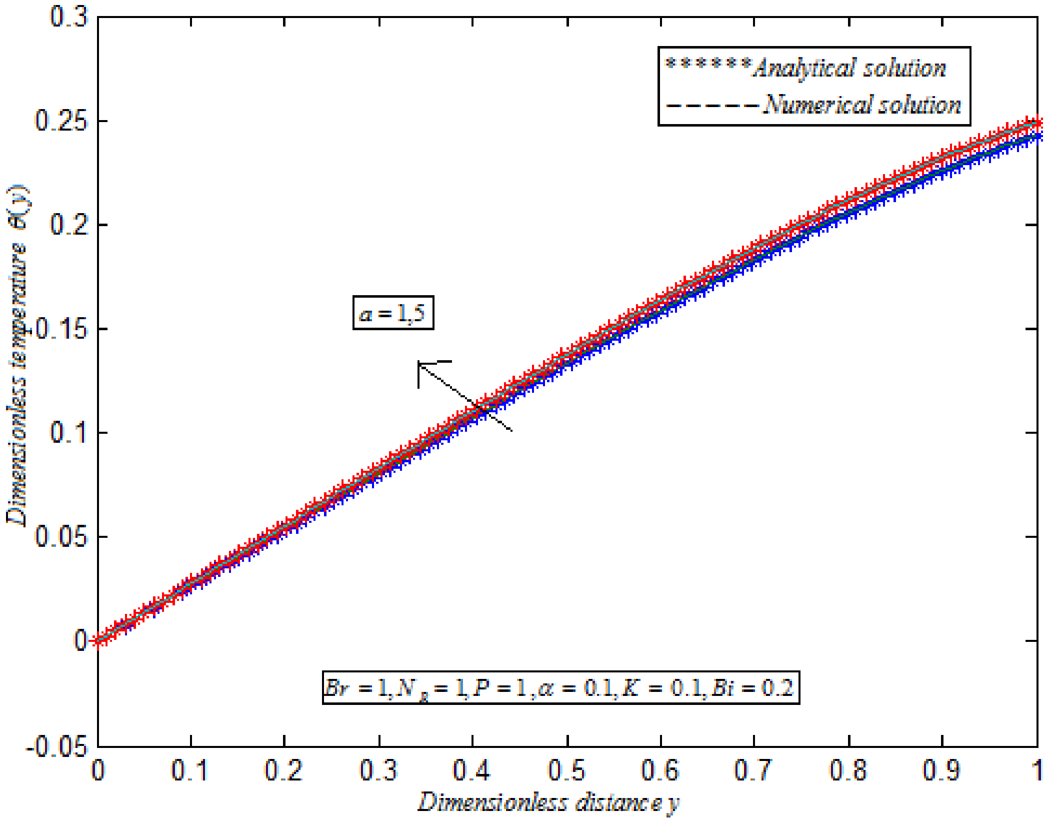

Figure 6. Dimensionless temperature $\theta(y)$ versus dimensionless distance *y*. The curves are plotted using the eqn. (52) for various values of the variable viscosity parameter a, and in some fixed values of the other dimensionless parameters $P, N_R, Br, \alpha, Bi, K$.

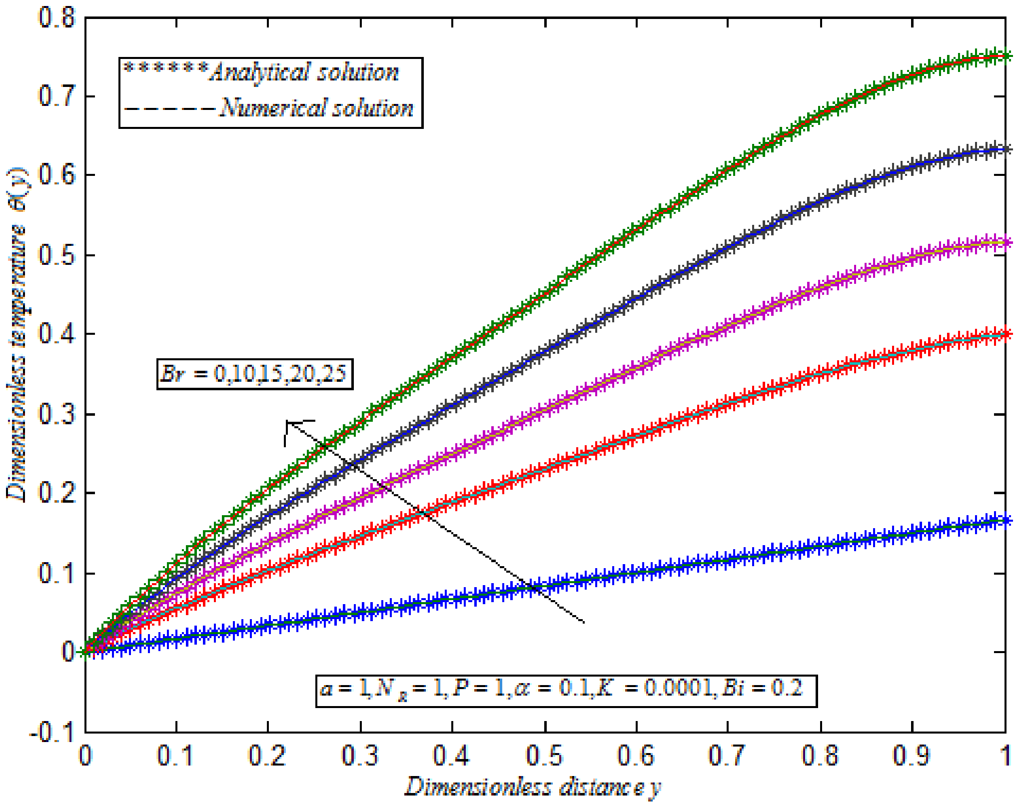

Figure 7. Dimensionless temperature $\theta(y)$ versus dimensionless distance *y*. The curves are plotted using the eqn. (52) for various values of the Brinkman number *Br*, and in some fixed values of the other dimensionless parameters N_R, P, a, K, α, Bi.

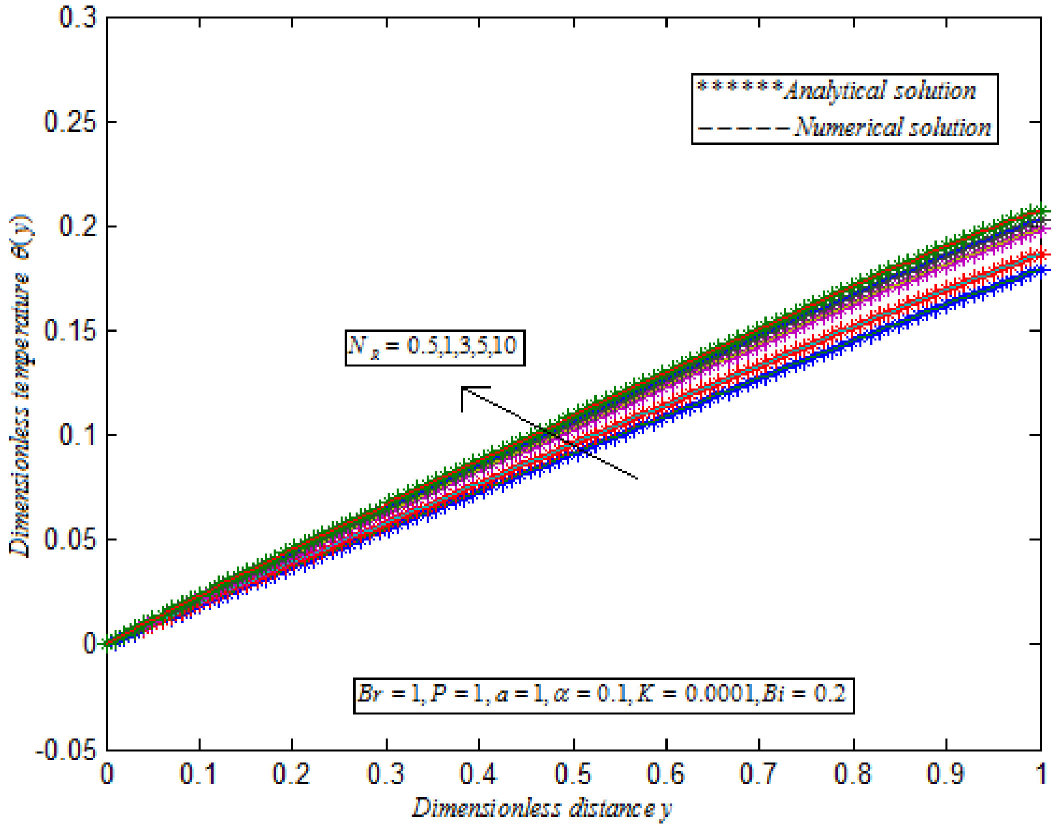

Figure 8. Dimensionless temperature $\theta(y)$ versu*s dimensionless* distance *y*. The curves are plotted using the eqn. (52) for various values of the Stark number N_R, and in some fixed values of the other dimensionless parameters *a, Br, P, K, Bi,* α .

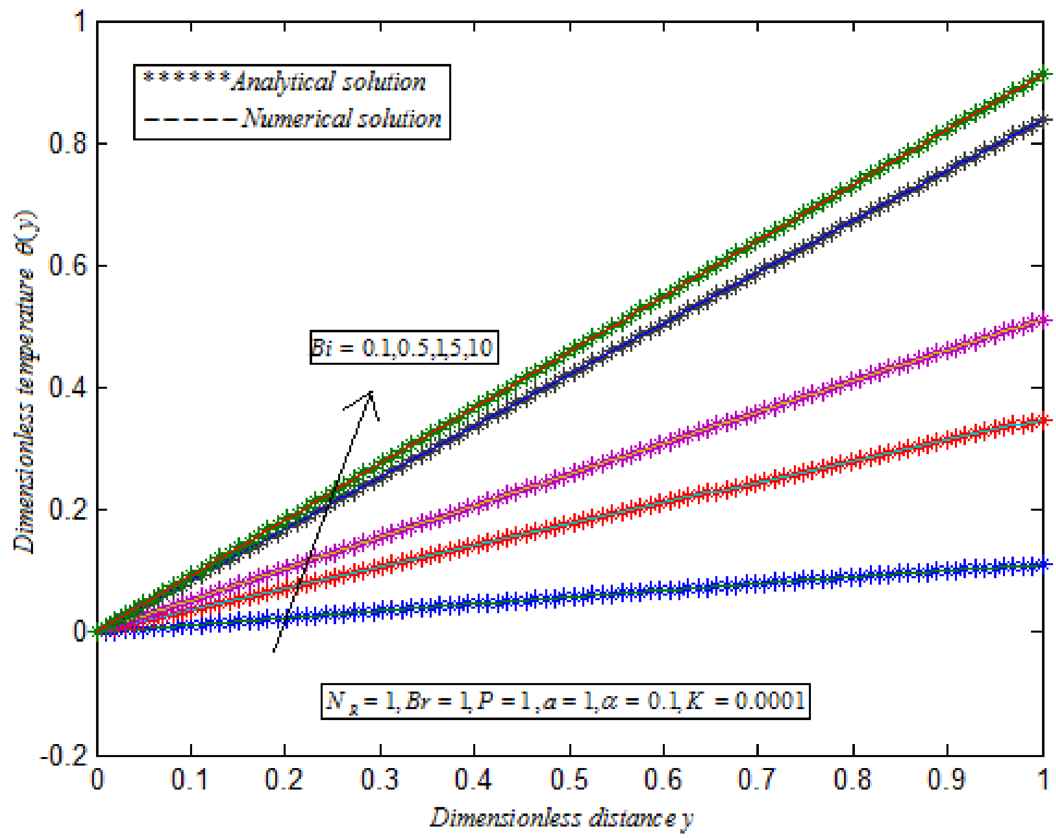

Figure 9. Dimensionless temperature $\theta(y)$ versus dimensionless distance *y.* The curves are plotted using the eqn. (52) for various values of the Biot number *Bi*, and in some fixed values of the other dimensionless parameters *a, Br, P, K,* N_R*,* α .

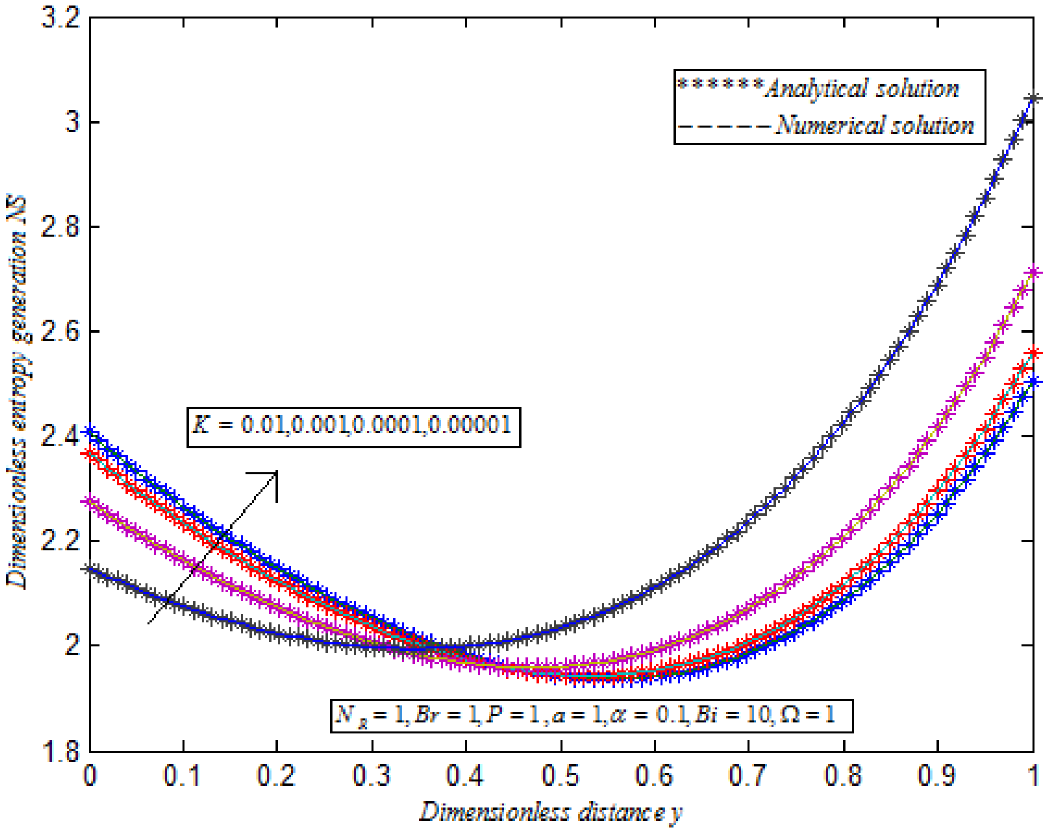

Figure 10. Dimensionless entropy generation *NS* versus dimensionless distance*y*. The curves are plotted using the eqns. (15), (56) and (16) for various values of the Permeability parameter *K*, and in some fixed values of the other dimensionless parameters *a, Br, P, Bi*, N_R, α , Ω .

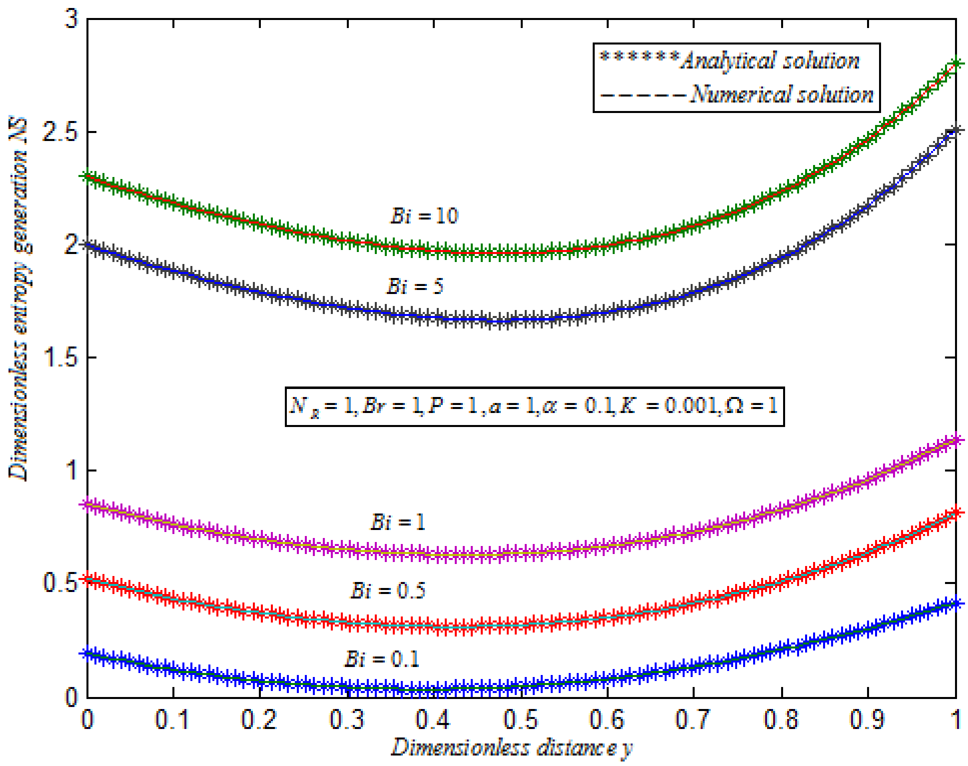

Figure 11. Dimensionless entropy generation *NS* versus dimensionlessdistance *y*. The curves are plotted using the eqns. (55), (56) and (16) for various values of the Biot number *Bi*, and in some fixed values of the other dimensionless parameters *a, Br, P, Bi*, N_R, α , Ω .

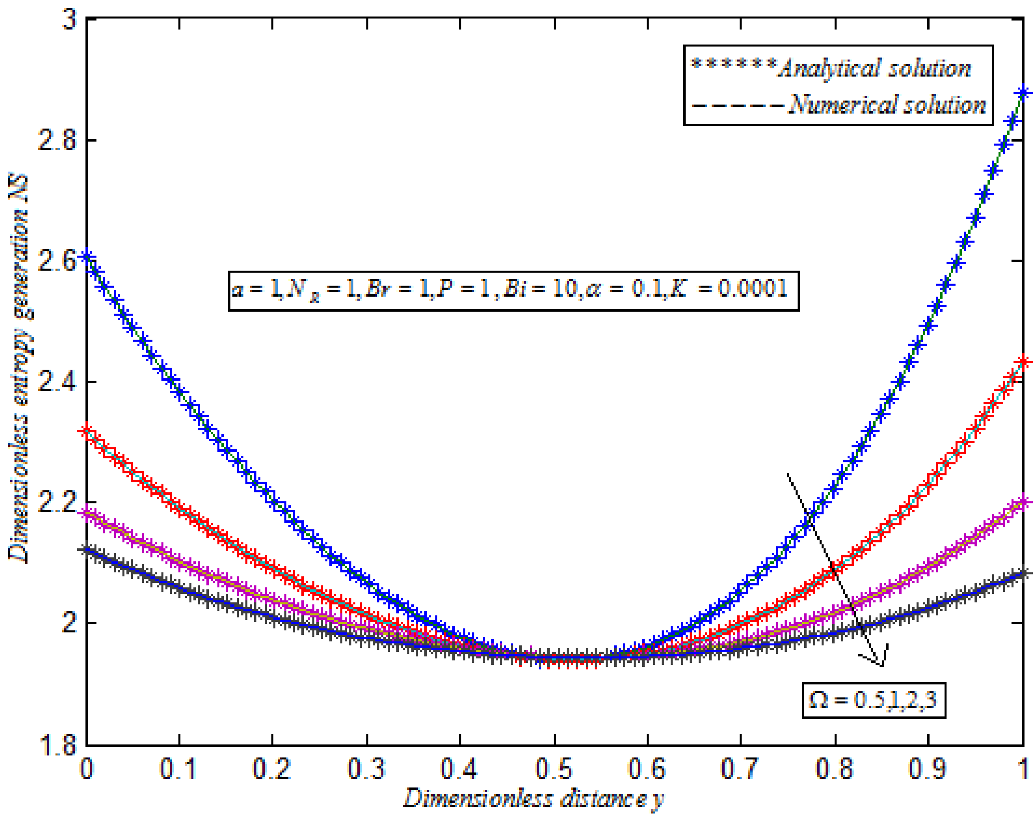

Figure 12. Dimensionless entropy generation *NS* versus dimensionless distance *y*. The curves are plotted using the eqns. (55) (56) and (16) for various values of the dimensionless temperature difference Ω , and in some fixed values of the other dimensionless parameters *a, Br, K, P, Bi,* N_R, α .

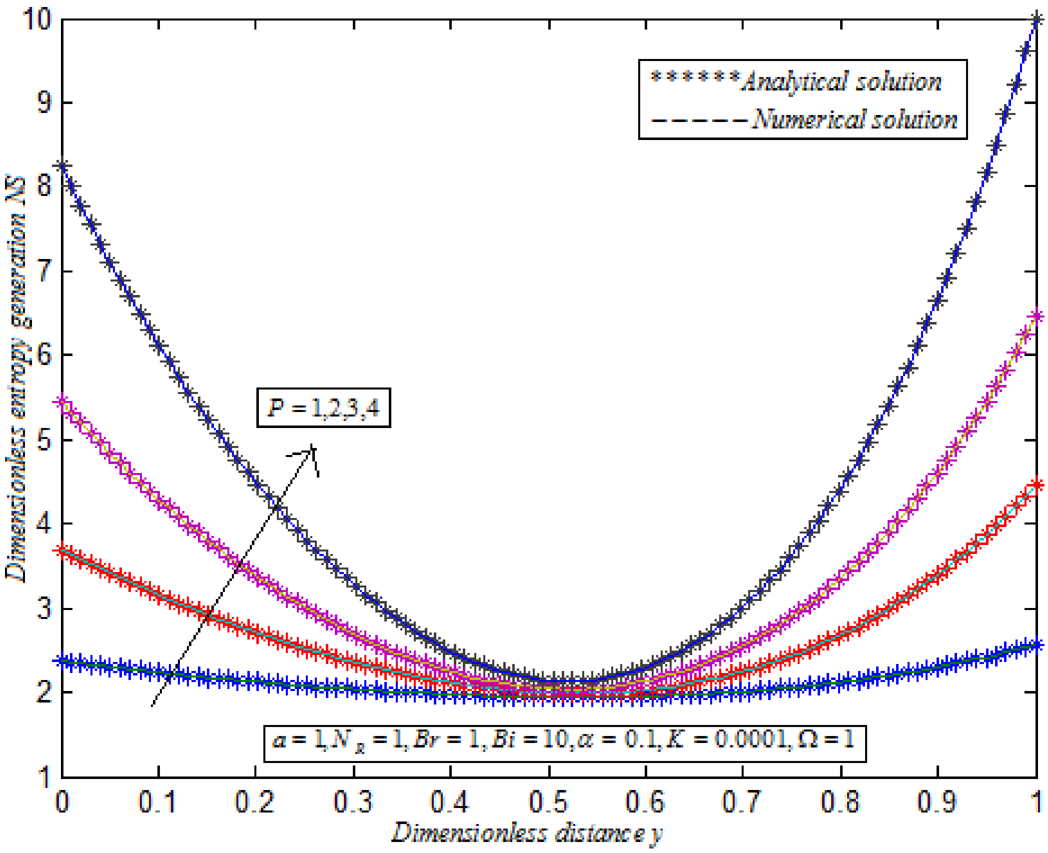

Figure 13. Dimensionless entropygeneration *NS*versus dimensionless distance *y*. The curves are plotted using the eqns. (55), (56) and 16) for various values of the non dimensional axial pressure gradient *P*, and in some fixed values of the other dimensionless parameters *a, Br, K,* θ, *Bi,* N_R, α .

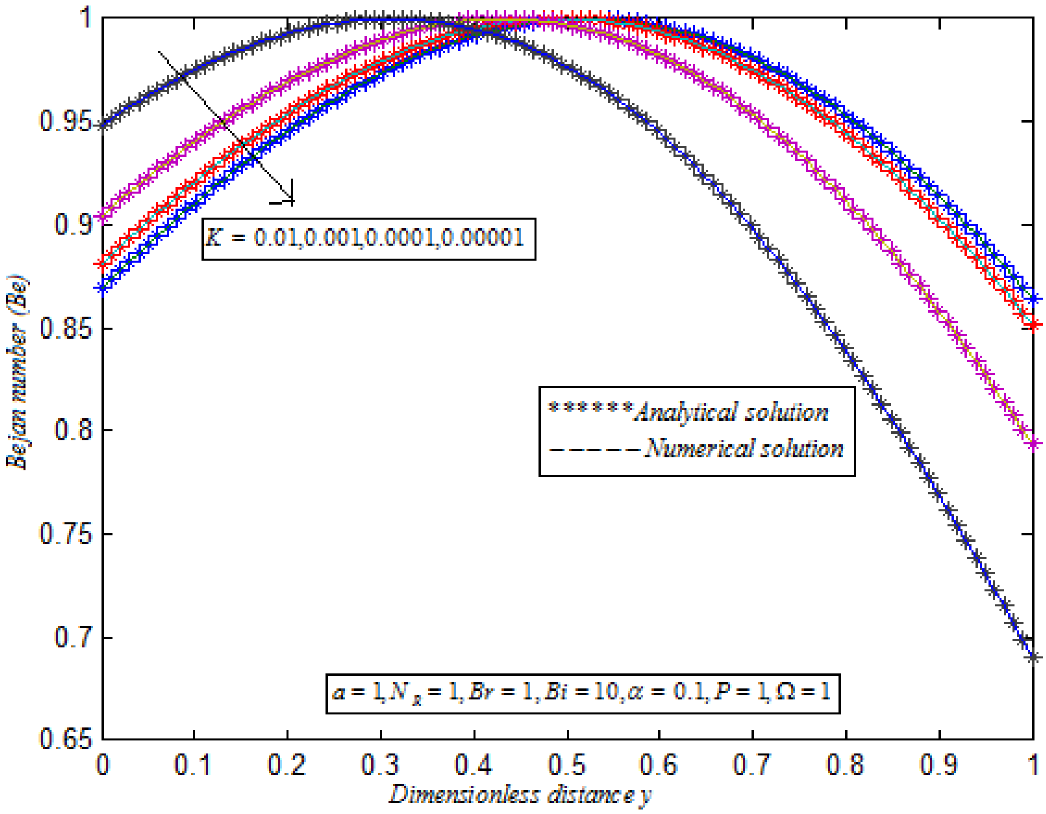

Figure 14. Bejan number *(Be)* versus dimensionless distance *y*. The curves are plotted using the eqns. (55), (56) and (17) for various values of the Permeability parameter *K*, and in some fixed values of the other dimensionless parameters *a, Br, P,* Ω *, Bi,* N_R*,* α .

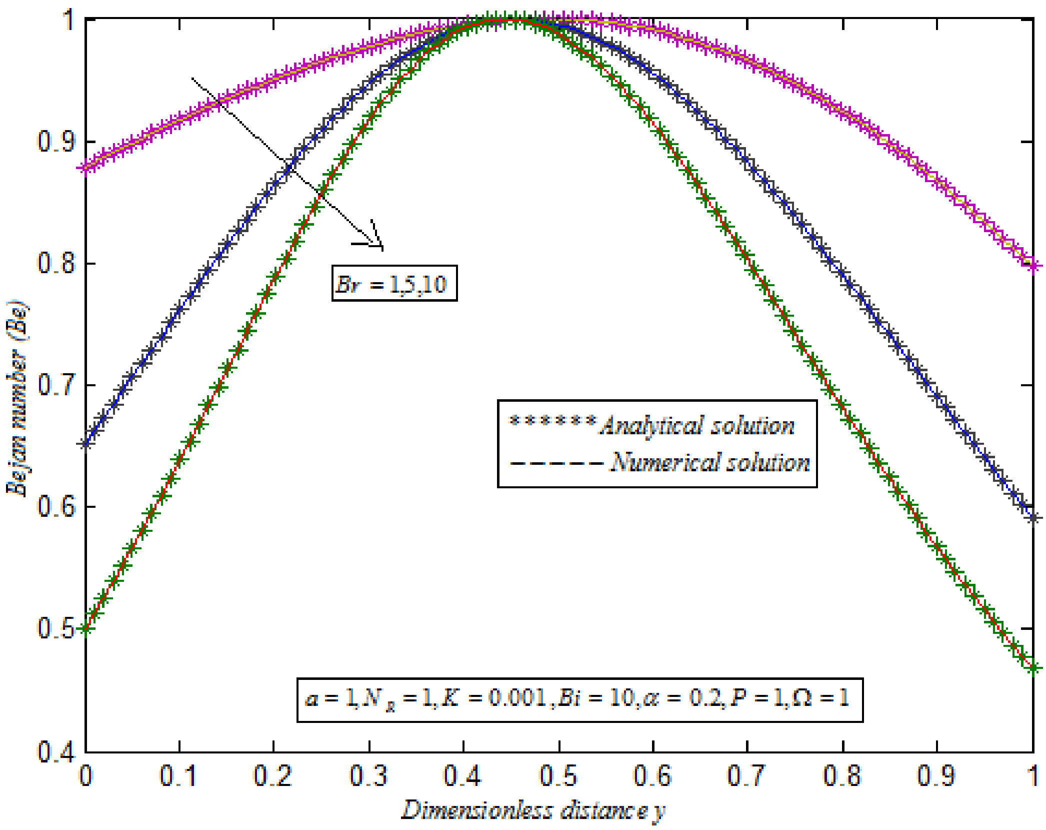

Figure 15. Bejan number *(Be)* versus dimensionless distance *y*. The curves are plotted using the eqns. (55), (56) and (17) for various values of the Brinkman number *Br*, and in some fixed values of the other dimensionless parameters *a, K, P,* Ω *, Bi,* N_R*,* α .

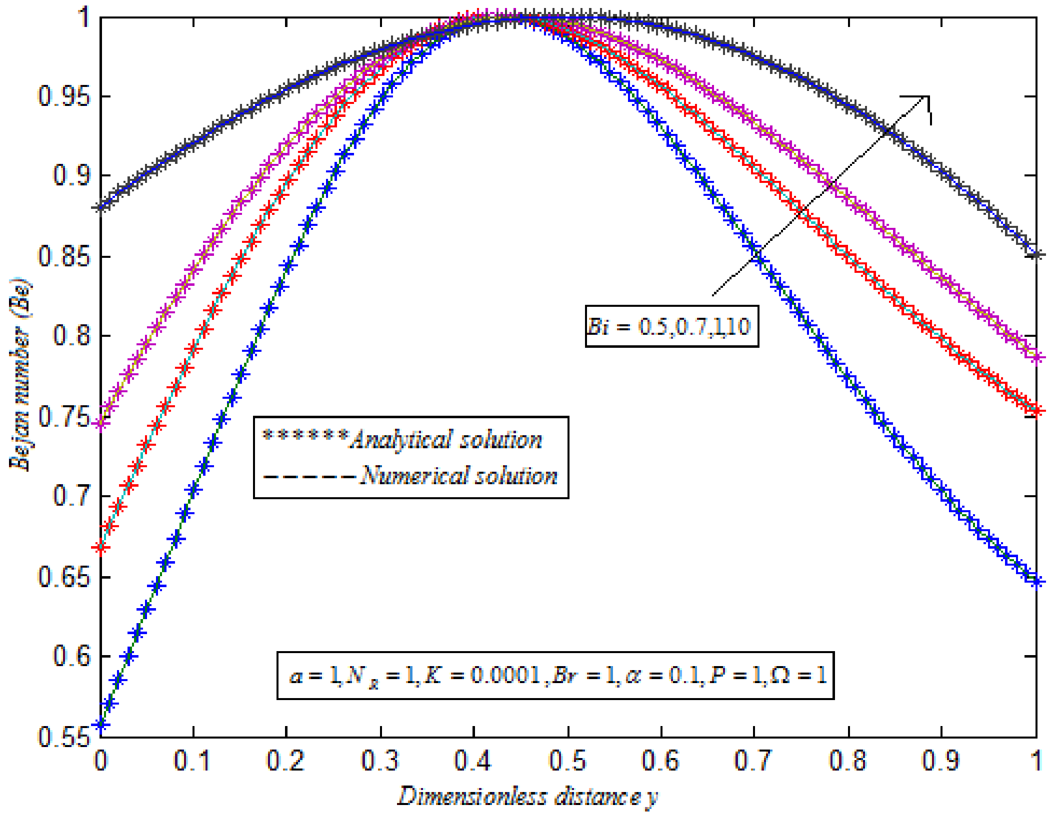

Figure 16. Bejannumber *(Be)* versus dimensionless distance *y*. The curves are plotted using the eqns. (55), (56) and (17) for various values of the Biot number *Bi*, and in some fixed values of the other dimensionless parameters *a, K, P,* Ω *, Br,* N_R, α .

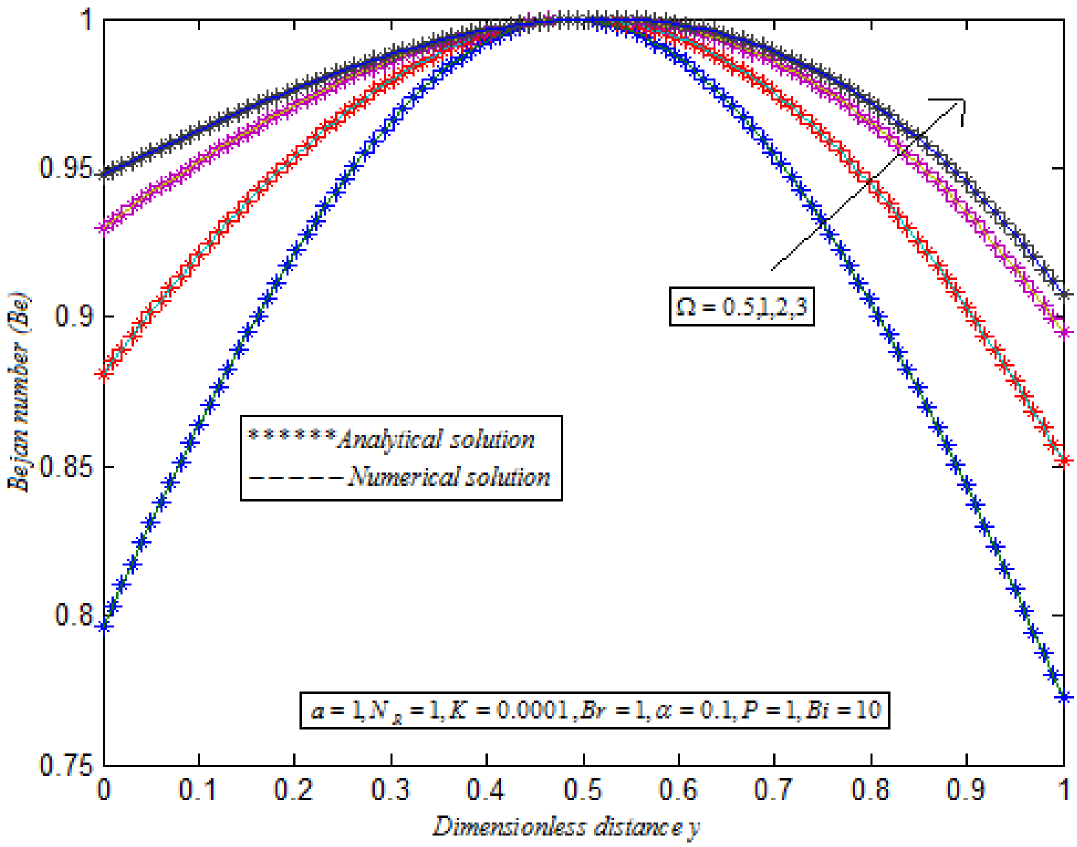

Figure 17. Bejan number *(Be)* versus dimensionless distance *y*. The curves are plotted using the eqns. (55), (56) and (17) for various values of the dimensionless temperature difference Ω , and in some fixed values of the other dimensionless parameters *a, K, P, Bi, Br,* N_R, α .

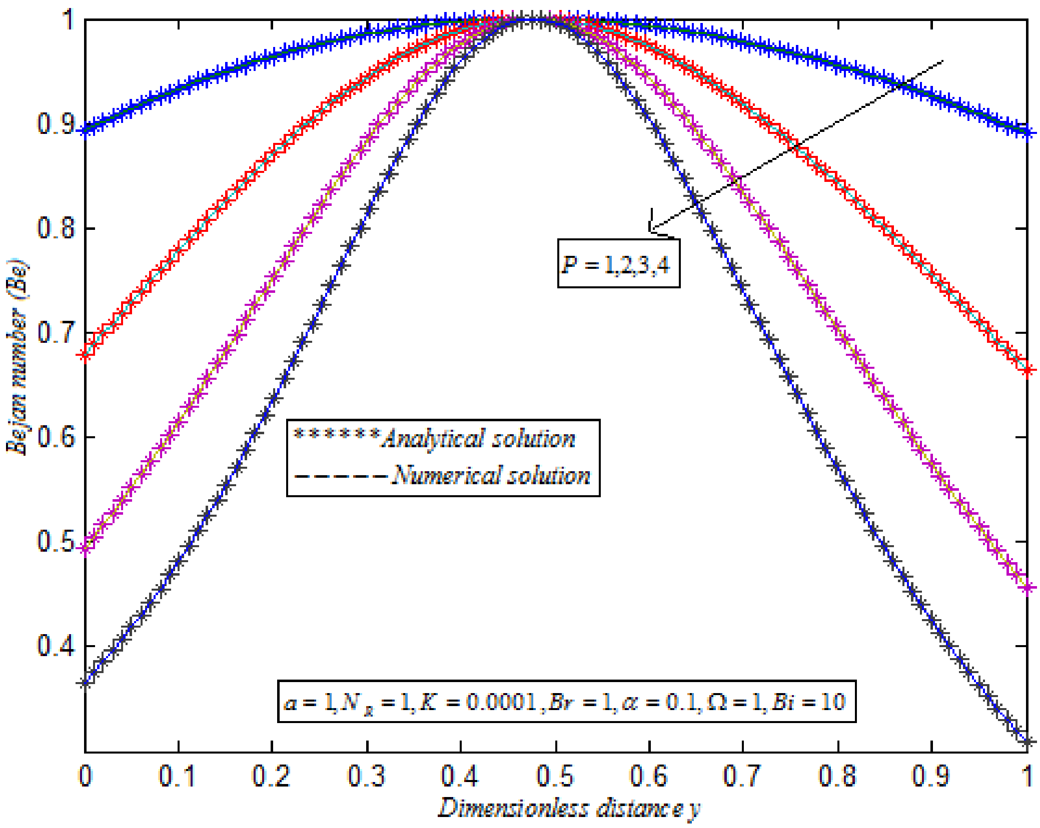

Figure 18. Bejan number *(Be)* versus dimensionless distance *y*. The curves are plotted using the eqns. (55), (56) and (17) for various values of the non dimensional axial pressure gradient *P*, and in some fixed values of the other dimensionless parameters *a, K,* Ω *, Bi, Br, N_R* and α .

5. Conclusion

In this paper the Homotopy analysis method is employed to get the analytical expression for theentropy generation in the Poiseuille flow of a temperature dependent viscosity through a channel. The approximate analytical expressions of the dimensionless velocity and dimensionless temperature profiles are derived mathematically and graphically using the Homotopy analysis method. The dimensionless entropy generation number and dimensionless Bejan number are also derived using the analytical expressions for the dimensionless velocity and dimensionless temperature profiles. We also derived the mathematical and graphical representations of the entropy generation number and the Bejan number. The Homotopy analysis method can be easily extended to solve the other non-linear boundary value problems in physical and chemical sciences.

Nomenclature

Symbols	Meaning
T_0	Constant temperature
T_1	Temperature
d	Width of channel
h	Heat transfer coefficient
μ_0	Viscosity of the fluid at T_0
λ	Viscosity variation parameter

$\bar{u}$	Velocity in the x-direction
T	Fluid temperature
ρ	Fluid density
C_P	The specific heat
k	Thermal conductivity
$-\frac{\partial \bar{p}}{\partial \bar{x}}$	Pressure gradient
$\mu(T)$	Temperature dependent viscosity of the fluid
$\bar{K}$	Permeability of the porous medium
α	Dimensionless constant
σ	Stefan-Boltz constant
k_1	Mean absorption coefficient
P	Dimensionless axial pressure gradient
U	Flow characteristic velocity
a	Variable viscosity parameter
T'	Reference temperature
NS	Dimensionless entropy generation number
NS_1	Dimensionless entropy generation due to heat transfer
NS_2	Dimensionless entropy generation due to fluid friction
Be	Bejan number
N_R	Stark number
Br	Brinkman number
Bi	Biot number
K	Permeability parameter
Ω	Dimensionless temperature difference

References

[1] D. S. Chauhan and V. Khemchandani, Entropy generation in the poiseuille flow of a temperature dependent viscosity fluid through a channel with a naturally permeable wall under thermal radiation, Advances in Applied Science Research., 7 (4) (2016), 104-120.

[2] D. A. Nield, and A. Bejan, Convection in Porous media 3rd edn, Springer, 2006.

[3] M. Chang, F. Chen and B. Straughan, Instability of poiseuille flow in a fluid overlying a porous layer, J. Fluid Mech., 64 (2006), 287-303.

[4] A. A. Hill, and B. Straughan, Poiseuille flow in a fluid overlying a porous medium, J. Fluid Mech., 603 (2008), 137-149.

[5] G. S. Beavers, and D. D. Joseph, Boundary conditions at a naturally permeable wall, J. Fluid Mech., 30 (1967), 197-207.

[6] P. G. Saffman, On the boundary condition at the surface of a porous medium, Stud. Appl. Math., 50 (1971), 93-101.

[7] A. J. Ochoa-Tapia, and S. Whitaker, Momentum transfer at the boundary between a porous medium and a homogeneous fluid, Int. J. Heat mass transfer, 38 (14) (1995a), 2635-2646.

[8] A. J. Ochoa-Tapia, and S. Whitaker, Momentum transfer at the boundary between a porous medium and a homogeneous fluid, Int. J. Heat mass transfer., 38 (14) (1995b), 2647-2655.

[9] D. F. James, and A. M. J David, Flow at the interface of a model fibrous medium, J. fluid Mech., 426 (2001), 47-72.

[10] D. S. Chauhan, and K. S. Shekhawat, Heat transfer in coquette flow of a compressible Newtonian fluid in the presence of a naturally permeable boundary, J. Phys. D: Appl. Phys., 26 (6) (1993), 933-936.

[11] D. S Chauhan, and P. Vyas, Heat transfer effects in a coquette flow through a composite channel partly filled by a porous medium with a transverse sinusoidal injection velocity and heat source, ASCE Journal of Engineering Mechanics., 121 (1) (1995), 57-61.

[12] A. V. Kuznetsov, Analytical investigation of the fluid flow in the interface region between a porous medium and a clear fluid in channels partially filled with a porous medium, Appl. Sci. Res., 56 (1996), 53-67.

[13] A. V. Kuznetsov, Analytical investigation of the fluid flow in the interface region between a porous medium and a clear fluid in channels partially filled with a porous medium, Int. J. of Heat and Mass Trransfer., 41 (1998), 2556-2560.

[14] A. V. Kuzenetsov, Fluid flow and heat transfer analysis of coquette flow in a composite duct, Acta Mech., 140 (3-4) (2000), 163-170.

[15] M. K. Alkam, M. A. Al-Nimir, and M. O. Hamdan, On forced convection in channels partially filled with porous substracts, 38 (2002), 337-342.

[16] M. A. Al-Nimir, and A. F. Khadrawi, Transient free convection fluid flow in domains partially filled withporous media, Transport in porous Media., 51 (2003), 157-172.

[17] A. Bejan, The new thermodynamics of finite-size devices and finite-time process, Entropy Generation minimization. CRC Press, New York, 1996.

[18] C. K. Chen, Y. T. Yang, and K. H. Chang, The effect of thermal radiation on entropy generation due to micro-polar fluid flow along a wavy surface, Entropy., 13 (2011), 1595-1610.

[19] S. J. Liao and K. F. Cheung, Homotopy analysis of nonlinear progressive waves in deep water, J. Engg. Maths., 45 (2003), 105-116.

[20] W. Kierkus, An analysis of laminar free convection flow and heat transfer about an inclined isothermal plate, Int. J. Heat mass trans., 11 (1968), 241-253.

[21] S. J. Liao, An explicit totally analytic approximation of Blasius viscous flow problems, Int. J. Non-Linear Mech., 34 (1999), 759-778.

[22] S. J. Liao and A. T. Chwang, Application of Homotopy analysis method in nonlinear oscillations, Trans. ASME: J. Appl. Mech., 65 (1998), 914-922.

[23] S. J. Liao, An analytical approximate technique for free oscillations of positively damped systems with algebraically decaying amplitude, Int. J. Non-Linear Mech., 38 (2003), 1173-1183.

[24] S. J. Liao, An analytic approximation of the drag coefficient for the viscous flow past a sphere. Int. J. Non-Linear Mech, 37 (2002), 1-18.

[25] S. J. Liao, The Homotopy Analysis method in non-linear differential equations. Springer and Higher Education Press. (2012), 45-54.

[26] S. J. Liao, Beyond Perturbation introduction to the Homotopy analysis method, First Edition, Chapman and Hall, CRC press, Boca Raton, (2003), 92-98.

[27] V. Ananthaswamy and S. UmaMaheswari, Analytical expression for the hydrodynamic fluid flow through a porous medium, International Journal of Automation and Control Engineering, 4 (2) (2015), 67-76.

[28] V. Ananthaswamy and L. SahanyaAmalraj, Thermal stability analysis of reactive hydromagnetic third-grade fluid using Homotopy analysis method, International Journal of Modern Mathematical Sciences, 14 (1) (2016), 25-41.

[29] V. Ananthaswamy and T. Iswarya, Analytical expressions of mass transfer effects on unsteady flow past an accelerated vertical porous plate with suction, Nonlinear studies. 23 (1) (2016), 73-86.

[30] V. Ananthaswamy and T. Iswarya, Analytical expressions of the effect of radiation on free convection flow of heat and mass transfer, Nonlinear studies, 23 (1) (2016), 133-147.

[31] F. C. Lai, and F. A. Kulacki, The effect of variable viscosity on convective heat transfer along a vertical surface in a saturated porous medium, Int. J. of Heat and Mass Transfer., 33 (1990), 1028-1031.

[32] R. Siegel and J. R. Howell, Thermal Radiation Heat Transfer, Int. Student Ed., McGraw Hill, New York, 1972.